

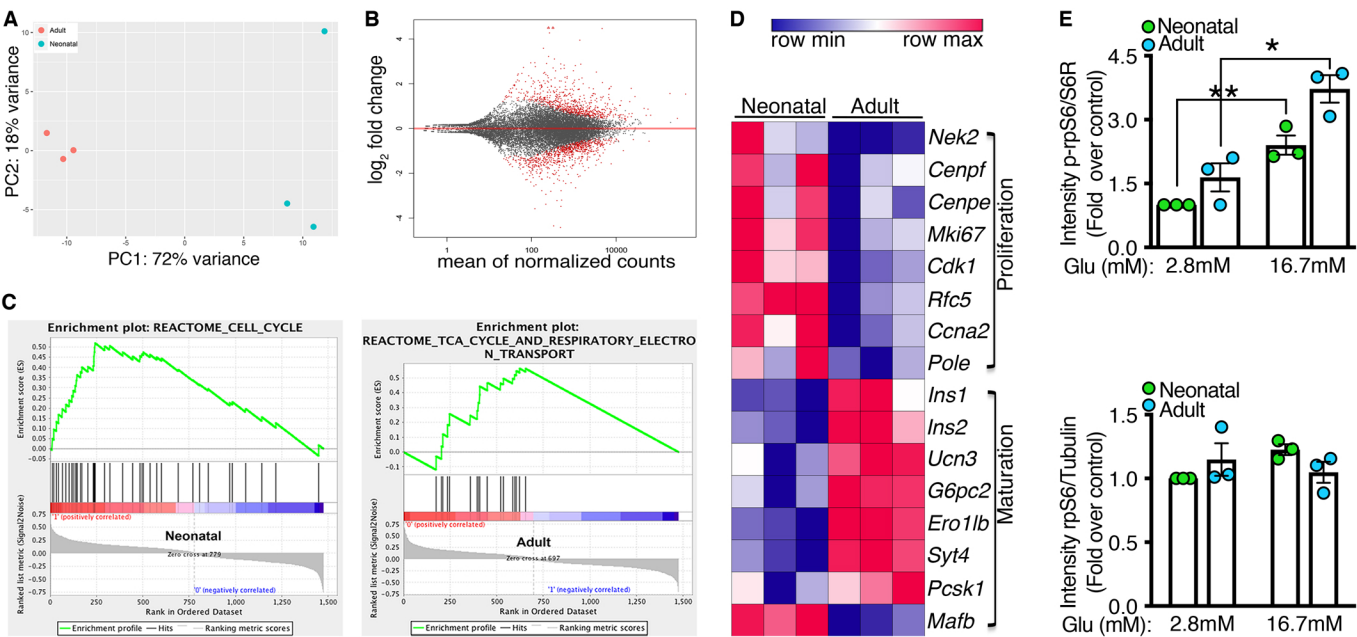
Supplemental Data

mTORC1 to AMPK Switching Underlies β -Cell Metabolic Plasticity During Maturation and Diabetes

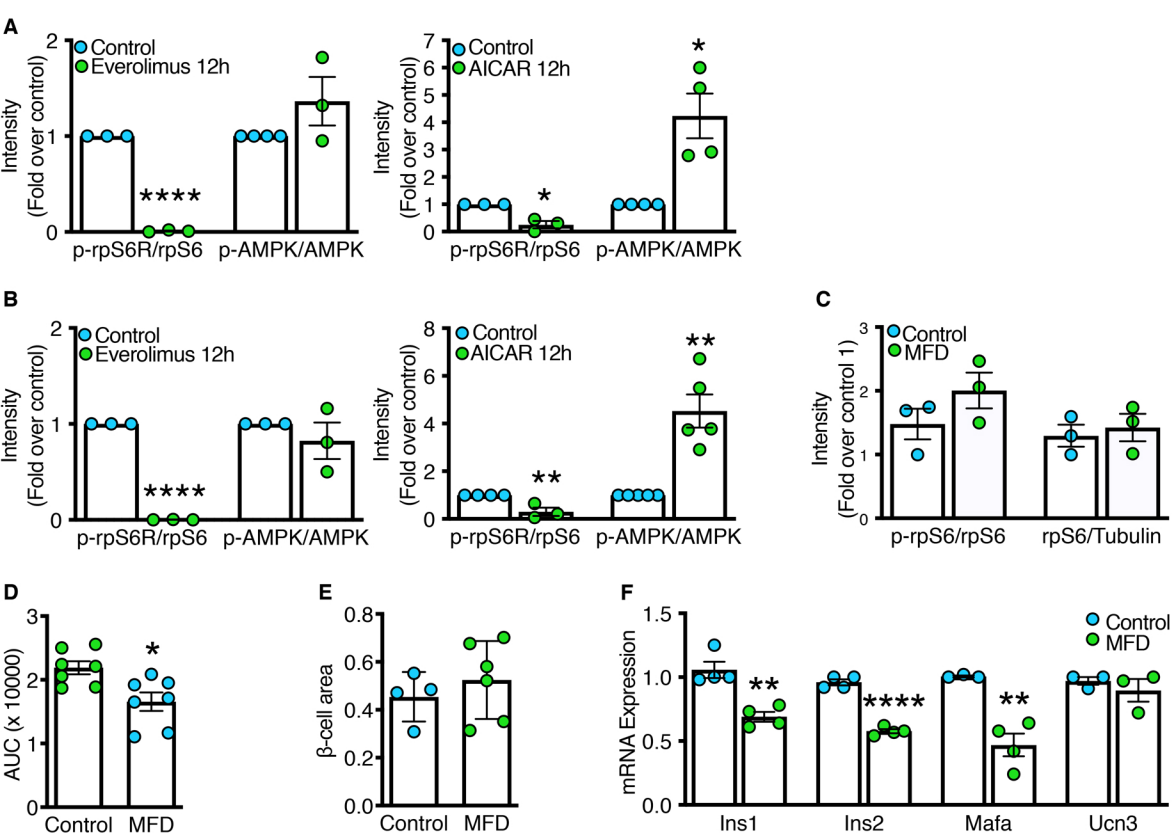
Rami Jaafar, Stella Tran, Ajit Shah, Gao Sun, Martin Valdearcos, Piero Marchetti, Matilde Masini, Avital Swisa, Simone Giacometti, Ernesto Bernal-Mizrachi, Aleksey Matveyenko, Matthias Hebrok, Yuval Dor, Guy A. Rutter, Suneil K. Koliwad*§, and Anil Bhushan*§.

* equal contribution.

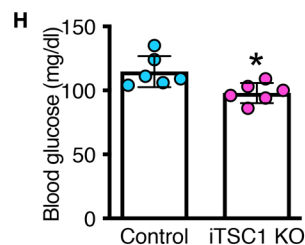
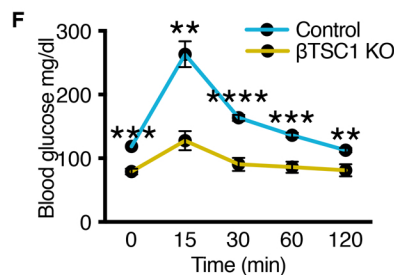
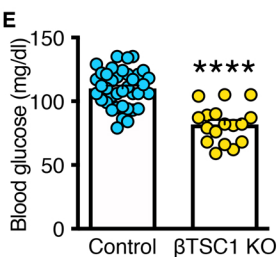
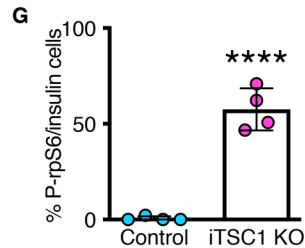
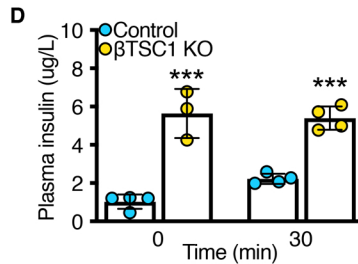
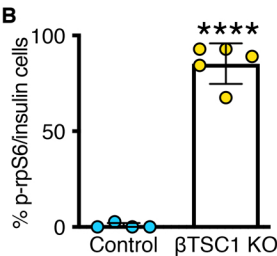
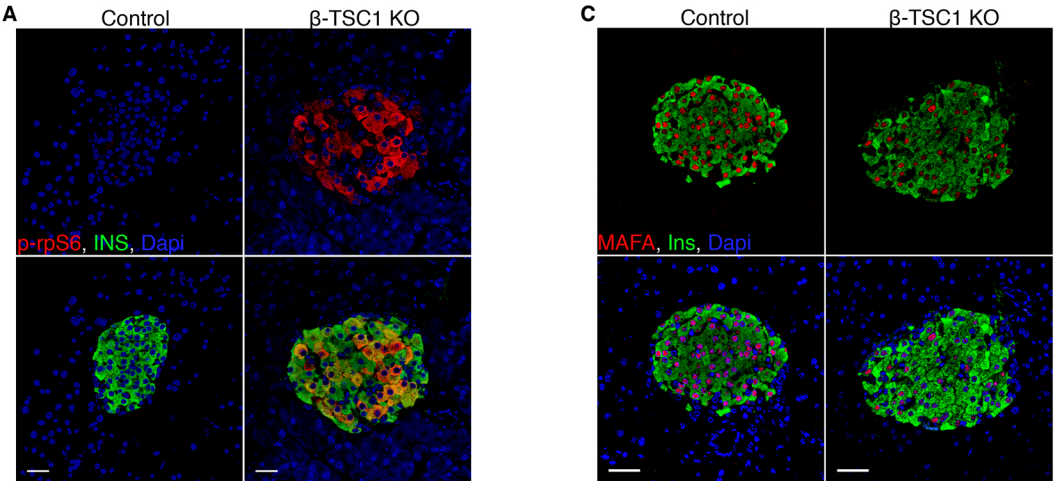
§ co-corresponding authors



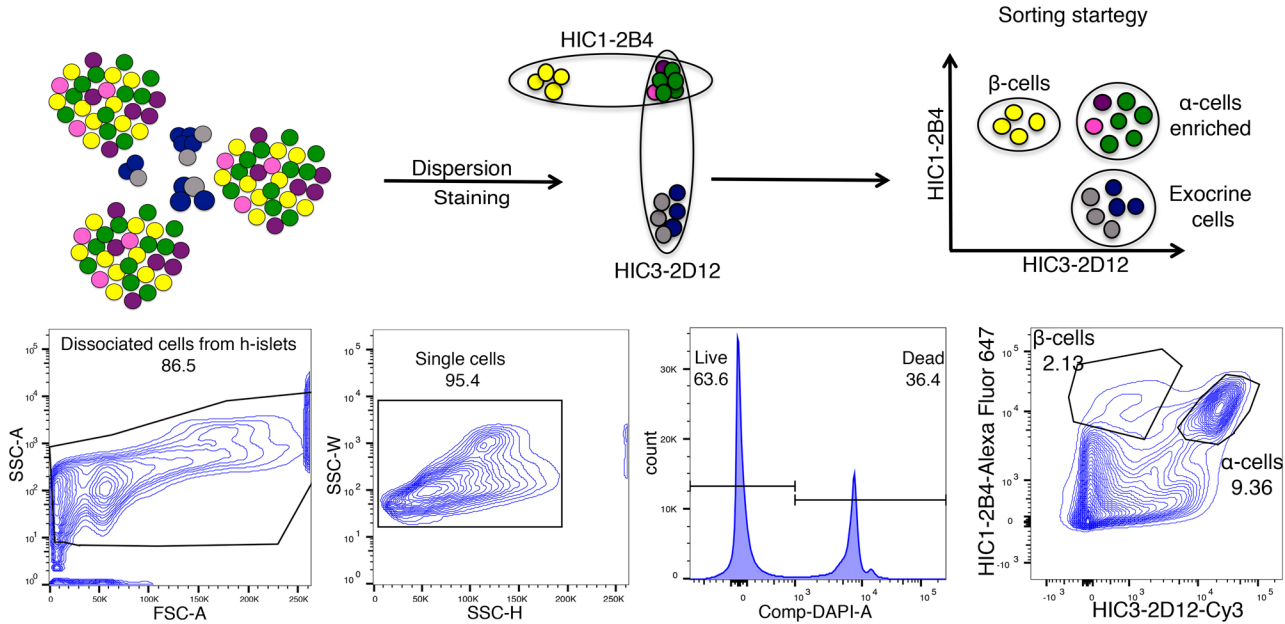
Supplemental Figure 1. A. Principal components analysis (PCA) of RNAseq libraries from P6 and P45 pancreatic β -cells. **B.** Plot of normalized mean expression counts vs. log₂-fold change for P6 vs. P45 β -cells. **C.** GSEA of RNAseq data, showing enrichment by reactome cell cycle pathway genes in neonatal β -cells, and instead, enrichment by reactome TCA cycle and respiratory electron transport chain genes in adult β -cells ($p < 0.05$). **D.** Heatmap, showing β -cell transcriptional profiles including relative upregulation of genes related to proliferation at P6 and maturation at P45 ($p < 0.05$). **E.** Quantification of data in Figure 1E, with p-rpS6 normalized to total rpS6 (top) and total rpS6 normalized to tubulin (bottom). ** $p = 0.006$ * $p = 0.0109$ (unpaired t-test corrected for multiple comparison using Holm-Sidak method).



Supplemental Figure 2. A. Quantification of the immunoblots in Figure 2A for p-rpS6 and p-AMPK performed on mouse islets treated for 12 hours with 40 μ M everolimus (left) or 1mM AICAR (right) normalized to total rpS6 or total AMPK, respectively (n=3 per group). * p= 0.0104, ****p < 0.0001 (unpaired t-test corrected for multiple comparison using Holm-Sidak method). **B.** Quantification of the immunoblots in Figure 2B for p-rpS6 and p-AMPK performed on human islets treated for 12 hours with 40 μ M everolimus (left) or 1mM AICAR (right) normalized to total rpS6 or total AMPK, respectively (n=3 per group). **p= 0.0051 ** p= 0.0018, and ****p < 0.0001 (unpaired t-test corrected for multiple comparison using Holm-Sidak method). **C.** Quantification of data in Figure 2D, showing p-rpS6 normalized to total rpS6 and total rpS6 normalized to tubulin. **D.** Figure 2E corresponding area under the curve n=7. *p= 0.011 (two-tailed unpaired t-test). **E.** Calculated β -cell area in islets from control mice and MFD mice (n=5-6). p= 0.4720 (two-tailed unpaired t-test). **F.** qPCR, showing relative mRNA levels of β -cell maturation markers in control and MFD mice n=3-4. **p= 0.008, ****p<0.0001 (unpaired t-test corrected for multiple comparison using Holm-Sidak method).



Supplemental Figure 3. A. Immunostaining for insulin (green), p-rpS6 (red), and DAPI (blue) in representative pancreatic sections from control and β -TSC1KO mice (scale bar: 50 μ m). **B.** Percentage of β -cells positive for both p-rpS6 and insulin in adult β -TSC1KO and control mice ($n=4-5$). **** $p<0.0001$ (two-tailed unpaired t-test). **C.** Immunostaining for insulin (green), MafA (red) and DAPI (blue) in representative pancreatic sections from adult β -TSC1KO and control mice (scale bar: 50 μ m). **D.** Plasma insulin levels after glucose challenge in β -TSC1KO and control mice ($n=5$), *** $p=0.0009$ and *** $p=0.00015$ (unpaired t-test corrected for multiple comparison using Holm-Sidak method). **E.** Fasting blood glucose levels in β -TSC1KO mice and littermate controls ($n=17-38$) **** $p<0.0001$ (two-tailed unpaired t-test). **F.** IPGTTs for β -TSC1 KO mice and littermate controls ($n=4-11$). ** $p<0.01$, **** $p<0.0001$, and **** $p<0.0001$ (unpaired t-test corrected for multiple comparison using Holm-Sidak method). **G.** Percentage of cells positive for both p-rpS6 and insulin in islets from iTSC1KO and control mice ($n=4$). **** $p<0.0001$ (two-tailed unpaired t-test). **H.** Fasting blood glucose levels in iTSC1KO mice and littermate controls ($n=6$). ** $p=0.0173$ (two-tailed unpaired t-test).



Supplemental Figure 4. Gating strategy for sorting β -cells from human islets.

Supplemental table 1

Log2 fold changes and associated p-value for genes presented in the heatmap shown in supplemental Fig 1D

Gene name	Log2 fold change	p-value
<i>Nek2</i>	-1.339034306	0.00941881
<i>Cenpf</i>	-0.977890623	0.03495696
<i>Cenpe</i>	-1.212366861	0.02397859
<i>Mki67</i>	-1.192655003	2.26E-005
<i>Cdk1</i>	-1.433178469	0.00792847
<i>Rfc5</i>	-1.528949667	0.00258173
<i>Ccna2</i>	-1.528532817	0.00103548
<i>Pol2</i>	-1.289185581	0.02712927
<i>Ins1</i>	1.566120644	2.68E-012
<i>Ins2</i>	1.540292745	5.16E-014
<i>Ucn3</i>	1.257778699	3.58E-006
<i>G6pc2</i>	1.425826996	5.60E-012
<i>Ero1b</i>	1.19744314	1.04E-016
<i>Syt4</i>	1.81888941	3.14E-016
<i>Pcsk1</i>	0.455240727	0.04116302
<i>Mafb</i>	-1.753123494	1.19E-016

Supplemental table 2

Log2 fold changes and associated p-value for genes presented in the heatmap shown in Figure 1B

Gene name	Log2 fold change	p-value
<i>Igf2</i>	-1.669744396	0.00535097
<i>Irs1</i>	-1.009097768	0.0049805
<i>Igf1r</i>	-1.009466088	3.26E-005
<i>Igf2bp1</i>	-3.584108315	3.16E-013
<i>Igf2bp2</i>	-2.420619212	1.32E-016
<i>Igf2bp3</i>	-4.351045752	1.71E-027
<i>Eif4g1</i>	-0.496406801	0.00311579
<i>Eif3b</i>	-0.518685897	0.0341385
<i>Eif4h</i>	-0.614698641	0.00934488
<i>Eif4a3</i>	-0.701346773	0.01070156
<i>Eif4a1</i>	-0.867112366	0.01129465
<i>Rps6ka2</i>	-0.466920254	0.0290266
<i>Foxo1</i>	-0.709903032	0.01876581
<i>Prkaa2</i>	1.951447958	5.23E-005
<i>Pten</i>	0.58453832	0.00173429

Supplemental table 3

Log2 fold changes and associated p-value for genes presented in the heatmap shown in Figure 3E

Gene name	Log2 fold change	p-value
<i>Ins1</i>	-3.738244171	8.72E-37
<i>Ins2</i>	-5.099994098	6.81E-54
<i>Ucn3</i>	-2.693629409	1.66E-14
<i>G6pc2</i>	-3.299783607	1.94E-28
<i>Ero1lb</i>	-2.875381609	2.53E-21
<i>Syt4</i>	-3.447526233	7.78E-15
<i>Pcsk1</i>	-2.47241789	4.60E-08
<i>Mafa</i>	-2.5436652	1.14E-05

Supplemental table 4

Log2 fold changes and associated p-value for genes presented in the heatmap shown in Figure 4A

Gene name	Log2 fold change	p-value
<i>mt-Co1</i>	0.901261886	1.66E-005
<i>mt-Co2</i>	1.257060123	0.00234427
<i>mt-Co3</i>	0.70901422	0.01370815
<i>mt-Cytb</i>	1.133039722	2.56E-006
<i>mt-Nd1</i>	0.896537131	0.01299598
<i>mt-Nd2</i>	0.749238012	0.03711852
<i>mt-Nd4</i>	1.150902649	0.00212917
<i>mt-Nd5</i>	0.848395287	0.00056296
<i>mt-Atp6</i>	0.980945583	0.0206238
<i>Atp5e</i>	1.478860056	0.00308137
<i>Atp6ap1</i>	0.622265079	0.01749909
<i>Cox5b</i>	0.809685423	0.01566565
<i>Cox6a2</i>	2.706722493	4.16E-008
<i>Cox7b</i>	1.048435595	0.00300421
<i>Cyb5a</i>	0.865927615	0.00806819
<i>Ndufa3</i>	1.294458592	0.02502589
<i>Uqcrh</i>	1.231889143	0.00128698
<i>Uqcrq</i>	1.226963434	1.30E-005

Supplemental table 5

Log2 fold changes and associated p-value for genes presented in the heatmap shown in Figure 4E

Gene name	Log2 fold change	p-value
<i>mt-Co1</i>	-0.868310802	1.18E-11
<i>mt-Co2</i>	-0.911171573	1.18E-12
<i>mt-Co3</i>	-0.880341761	1.29E-25
<i>mt-Nd1</i>	-0.726717508	6.48E-08
<i>mt-Nd2</i>	-0.937632202	3.18E-12
<i>mt-Nd4</i>	-0.95314497	1.21E-13
<i>mt-Nd5</i>	-1.010724448	2.41E-16
<i>mt-Atp6</i>	-0.90594167	5.55E-22
<i>Atp8</i>	-0.844959725	2.59E-14
<i>Atp2a2</i>	-0.473449972	0.00017864
<i>Atp6ap2</i>	-0.611224628	3.96E-10
<i>Atp6v1e1</i>	-0.45885391	5.04E-09
<i>Atp6v1d</i>	-0.486891211	2.99E-24
<i>Cox7a2l</i>	-0.506881364	0.0003437
<i>Cox6a2</i>	-0.722191874	0.0003903
<i>Ppargc1a</i>	-0.523333512	0.039
<i>Ppargc1b</i>	-0.397202902	0.06413312

Supplemental table 6

Log2 fold changes and associated p-value for genes presented in the heatmap shown in Figure 5A

Gene name	Log2fold change	p value
<i>mTor</i>	0.780377302	0.01287027
<i>Akt1</i>	0.705019398	0.00125506
<i>Igf1r</i>	0.970627039	0.00736922
<i>Igf2r</i>	1.438017002	1.76E-09
<i>Rps6ka1</i>	1.20304205	0.00902307
<i>Rps6ka2</i>	0.618403979	0.04289504
<i>Rps6ka4</i>	0.919014983	0.00025866
<i>Pdk1</i>	1.094459248	0.00210561
<i>Eif4a3</i>	0.938303261	0.00085781
<i>Eif4ebp1</i>	1.63063821	3.61E-07
<i>Eif4g1</i>	0.508975641	0.02180279
<i>Eif4h</i>	0.474795353	0.04136719
<i>Eif4b</i>	1.188249422	4.29E-07
<i>Eif4a3</i>	0.938303261	0.00085781
<i>Pik3r5</i>	2.298347767	1.41E-07
<i>Ulk1</i>	1.155388941	3.27E-06
<i>Ambra1</i>	0.7668819	0.00379013
<i>Rptor</i>	1.162070397	8.44E-06
<i>Prkaa1</i>	-0.887260688	0.00629938
<i>Ppp2ca</i>	-1.251862877	8.82E-07
<i>Fkbp1a</i>	-0.665205399	0.0046429
<i>Fkbp1b</i>	-2.189758461	2.40E-21
<i>Mapk1</i>	-0.759869661	0.00323474
<i>Ins2</i>	-0.864623497	0.00080844
<i>Ucn3</i>	-1.093252337	6.26E-06
<i>G6pc2</i>	-0.877497222	0.00241343
<i>Ero1b</i>	-1.817987497	5.89E-22
<i>Pcsk1n</i>	-1.257182893	2.31E-08

Supplemental table 7: qPCR primer sequences

	Forword primer	Reverse primer
PGC1a	GAATCAAGCCAGTACAGACACCG	CATCCCTCTTGAGCCTTTCGTG
PGC1b	CAGCCTCAGTTCCAGAAGTCAG	CACCGAAGTGAGGTGCTTATGC
Ins1	AGGACCCACAAGTGGAACAAC	GTGCAGCACTGATCCACAATG
Ins2	GCTCTCTACCTGGTGTGTGGG	CTCCACCCAGCTCCAGTTGTG
Ucn3	AAGCCTCTCCCACAAGTTCTA	GAGGTGCGTTTGGTTGTCATC
Glut2	GTTGGAAGAGGAAGTCAGGGCA	ATCACGGAGACCTTCTGCTCAG
Mafa	TCAGCAAGGAGGTCATCCGA	TGGCTCTGGAGCTGGCACTTCT

Supplemental table 8: list of disallowed genes.

Pullen et al.2010		
HBA	BLOC1S1	PFKL
NDRG2	C1qBP	PFKP
HBB	CAT	H6PD
SLC16A1	CD302	PGD
ABCA8A	COX5A	RPE
MYL9	CRLZ1	ACLY
LY6A	CXCL12	ACSS2
CAR2	FCGRT	HSD17b7
TST	HIGD1A	GDPD1
LY6C	IGFBP4	MVK
FXYD1	ISLR	SOAT1
SULT1A1	ITIH5	
GAS6	LDHA	
GDA	LMO4	
MGST3	MAF	
CXCL12	MCT1	
MGLL	MGST1	
GSTA4	MYLK	
LDHA	NOLA2	
PDGFRA	OAT	
TNS1	OGN	
OAT	PARP3	
FGF1	PCOLCE	
FAM59A	PDGFRA	
CD302	PRL24	
NFIB	PRL36	
DDAH1	SELENBP1	
ASPA	SMAD3	
CCL21	TGM2	
GAS1	UQCRB	
ACOT7	ZFP36L1	
NDRG4	ZYX	
YAP1	DNMT3a	
GALM	HK1	
GUCY1A3	HK2	
PLEC1	LDHA	
AK3	ALDOB	
ZDHHC9	TPI1	
IGFBP4	PGM1	
ZFP622	PGM2	
ARHGDIB	BPGM	

Thorrez et al. 2011
ZFP622
ARHGDIB
BLOC1S1
C1qBP
CAT
CD302
COX5A
CRLZ1
CXCL12
FCGRT
HIGD1A
IGFBP4
ISLR
ITIH5
LDHA
LMO4
MAF
MCT1
MGST1
MYLK
NOLA2
OAT
OGN
PARP3
PCOLCE
PDGFRA
PRL24
PRL36
SELENBP1
SMAD3
TGM2
UQCRB
ZFP36L1
ZYX

Dhawan et al. 2015
DNMT3a
HK1
HK2
LDHA
ALDOB
TPI1
PGM1
PGM2
BPGM
PFKL
PFKP
H [^] PD
PGD
RPE
ACLY
ACSS2
HSD17b7
GDPD1
MVK
SOAT1